Journal of Power Sources 195 (2010) 7734–7742

Contents lists available at ScienceDirect

Journal of Power Sources

journal homepage: www.elsevier.com/locate/jpowsour

New inorganic–organic proton conducting membranes based on Nafion and hydrophobic fluoroalkylated silica nanoparticles

Vito Di Noto[a,b,*,1], Nicola Boaretto[a], Enrico Negro[a], Giuseppe Pace[b]

[a] Dipartimento di Scienze Chimiche, Università di Padova, Via Marzolo 1, I-35131 Padova (PD), Italy
[b] Istituto di Scienze e Tecnologie Molecolari, ISTM-CNR and INSTM, Dipartimento di Scienze Chimiche, Via Marzolo 1, I-35131 Padova (PD), Italy

ARTICLE INFO

Article history:
Received 31 July 2009
Received in revised form
22 September 2009
Accepted 13 October 2009
Available online 31 October 2009

Keywords:
Hybrid inorganic–organic proton conducting membranes
Nafion
Polymer electrolyte membrane fuel cells
Dynamical mechanic analysis
Broadband dielectric spectroscopy

ABSTRACT

In this report, a new nanofiller consisting of silica "cores" bearing fluoroalkyl surface functionalities is synthesized and adopted in the preparation of a series of hybrid inorganic–organic proton conducting membranes based on Nafion. The hybrid materials are obtained by a solvent-casting procedure and include between 0 and 10 wt.% of nanofiller. The resulting systems are extensively characterized by Thermogravimetry (TG), Modulated Differential Scanning Calorimetry (MDSC) and Dynamic Mechanical Analysis (DMA), showing that the hybrid materials are stable up to 240 °C and that their overall thermal and mechanical properties are affected both by the polar groups on the surface of the silica "cores" and by the fluoroalkyl surface functionalities of the nanofiller. The electric properties of the hybrid materials are investigated by broadband dielectric spectroscopy (BDS). It is shown that proton conductivity of the materials is not compromised by the lower water uptake arising from the hydrophobic character of the nanofiller. With respect to a pristine Nafion recast membrane, the hybrid material characterized by 5 wt.% of nanofiller, [Nafion/$(Si_{80}F)_{0.7}$], shows the highest conductivity in all the investigated temperature range ($5 \leq T \leq 155$ °C). Indeed, [Nafion/$(Si_{80}F)_{0.7}$] features the lowest water uptake and presents a conductivity of 0.083 S cm^{-1} at 135 °C. This result is consistent with the good performance of the membrane in single fuel cell tests.

1. Introduction

Perfluorinated polymers such as Nafion, Aciplex, Flemion and the Dow polymer are crucial materials for the development of polymer electrolyte membrane fuel cells (PEMFCs) and direct methanol fuel cells (DMFCs) [1,2]. Major obstacles to a large-scale commercialization of PEMFCs based on these systems include the high cost of perfluorinated membranes, the poor proton conductivity at a low relative humidity (RH), and poor mechanical properties at $T > 130$ °C. In the case of Nafion, the drastic fall of the proton conductivity at high temperatures limits the practical utilization range of this material at temperatures of ca. 90 °C. To address these issues, inorganic–organic composite membranes based on Nafion and fillers with a size ranging from nanometers to micrometers have been intensively explored and remain one of the most interesting routes in the preparation of promising electrolytes for application in PEMFCs [3–13]. In particular, Nafion has been doped with heteropolyacids such as the phosphotungstic acid; the resulting system was used in PEMFCs which showed a good performance at low RH and high temperatures (ca. 120 °C) [5–7]. Nafion has also been doped with hygroscopic oxides such as SiO_2, TiO_2, ZrO_2, Al_2O_3 and others, to increase the water uptake of the membranes and to decrease the humidification requirements of the PEMFC [8–13]. In some cases hybrid membranes were prepared by sol–gel techniques [8–11]. The same approach was used to synthesize tailored organic-modified silica bearing a variety of functional groups, with a preference for hydrophilic fragments. The latter systems are devised to improve the proton conductivity and the water uptake of the resulting hybrid Nafion-based materials [14–17]. At present, the influence of the physicochemical properties of the inorganic fillers on the structure and the properties of the composite proton conducting polymer electrolytes is not well-understood and prompted us to investigate systematically composite Nafion-based membranes under different conditions. Thus, investigations were carried out on: (a) [Nafion/$(SiO_2)_x$] and [Nafion/$(HfO_2)_x$] nanocomposite membranes with $0 \leq x \leq 15$ wt.% [13,18]; (b) [Nafion/$(M_xO_y)_n$] membranes with M = Ti, Zr, Hf, Ta and W and $n = 5$ wt.% [19,20]; and (c) nanocomposite membranes of formula {Nafion/[$(M1_xO_y)\cdot(M2_aO_b)_c$]}, where M1 = Zr, Ti and M2 = Si, W [21,22]. These studies revealed that the mechanical, thermal and dynamic features of the Nafion host polymer depend on the concentration in the bulk material of

* Corresponding author at: Dipartimento di Scienze Chimiche, Università di Padova, Via Marzolo 1, I-35131 Padova (PD), Italy.
E-mail address: vito.dinoto@unipd.it (V. Di Noto).
[1] Active ACS, ECS and ISE member.

0378-7753/$ – see front matter © 2009 Elsevier B.V. All rights reserved.
doi:10.1016/j.jpowsour.2009.10.028

R–SO_3H···[filler]···HSO_3–R dynamic crosslinks, which are responsible for the good thermal, mechanical and electrical stability of the materials. It was shown that the electrical response of the hybrid membranes depends on the interactions occurring between the polar groups of Nafion and the filler; in addition, it was also revealed that the proton conduction mechanism of Nafion is modulated by the segmental motion of the fluorocarbon backbone chains [13]. The last observation prompted us to study the effect of the introduction in bulk Nafion of a hydrophobic filler. Indeed, it is expected that hydrophobic nanoparticles could interact preferentially with the fluorocarbon backbone chains of the host material. To the best of our knowledge, this approach is unexplored since it is believed that the conductivity of Nafion-based polymer electrolytes depends exclusively on the water retention capacity of the material. Thus, most of the efforts were aimed at increasing the water uptake of the materials, in particular by introducing in the membranes very hydrophilic nanofillers [4]. In this report, a hydrophobic nanofiller was prepared by a direct reaction between nanometer sized silica and a fluoroalkyloxirane, the (2,2,3,3,4,4,5,5,6,6,7,7,8,8,9,9,9-Heptadecafluorononyl)oxirane (HFNO). The modified silica thus prepared, named $Si_{80}F$, was then used to obtain a set of membranes with formula [Nafion/$(Si_{80}F)_\Psi$], where Ψ is the molar ratio of silicon atoms to sulfonic acid groups; its values range between 0 and 1.6. The composite membranes were characterized by TGA, MDSC, DMA and by broadband dielectric spectroscopy (BDS), in order to investigate the influence of the hydrofobic nanofiller on the thermal, mechanical and electrical properties of the materials. Finally, the best performing hybrid membrane was used to prepare a membrane-electrode assembly (MEA), which was tested in operating conditions. The performance of this later MEA was compared with that of a MEA assembled with Nafion reference material.

2. Experimental

2.1. Reagents

A 5 wt.% solution of Nafion ionomer (Ion Power Inc.) with a proton exchange capacity (PEC) of 1 mequiv. g^{-1} was used as received. Si_{80} amorphous silica was provided by Silysiamont S.p.A., Italy and was purified by standard methods [23]. (2,2,3,3,4,4,5,5,6,6,7,7,8,8,9,9,9-Heptadecafluorononyl)oxirane (HFNO), 96%, was purchased from Sigma–Aldrich and used as received. All the solvents were supplied by Aldrich and further purified by standard methods [23]. Bidistilled water was used in all procedures.

2.2. Nanofiller preparation and determination of proton exchange capacity (PEC)

Ca. 1 g of Si_{80} was milled for 10 h at 500 rpm in a tungsten carbide grinding jar using a planetary ball mill. The resulting powders were treated at room temperature for 1 h with H_2O_2, 36 vol.% and then with 2 M H_2SO_4. The product was rinsed with bidistilled water and dried at 100 °C under vacuum for 8 h. The hydrophobic nanofiller $Si_{80}F$ was prepared with the following procedure. The purified silica powders were added to ca. 10 mL of a HFNO/diethyl ether 50% (v/v) solution. This operation was carried out under N_2 atmosphere. The resulting suspension was stirred vigorously for 1 h; afterwards, ca. 20 μL of concentrated sulphuric acid were added. The product was stirred for 16 h at room temperature, washed several times with diethyl ether and then with methanol and finally dried at 100 °C under vacuum for 8 h. The proton exchange capacity (PEC) of Si_{80} and $Si_{80}F$ was determined as described elsewhere [13]. Briefly, an aliquot of each sample was suspended in a 1 M KCl solution and the product was allowed to equilibrate for 12 h. The PEC was measured by titrating the product with 1 mM KOH using phenolphthalein as an indicator.

Table 1
Composition of [Nafion/$(Si_{80}F)_\Psi$] membranes.

Nanofiller concentration (wt.%)	Ψ[a]	Nafion (g)	$Si_{80}F$ (mg)
0	0	0.45	0
3	0.4	0.45	13.9
5	0.7	0.45	23.7
7	1.0	0.45	33.9
10	1.6	0.45	50

[a] $\Psi = \frac{mol_{Si}}{mol_{-SO_3H}}$.

2.3. Membrane preparation

Five hybrid membranes with a nanofiller concentration ranging from 0 to 10 wt.% were prepared as follows. A suitable amount of the $Si_{80}F$ nanofiller (see Table 1) was added to a suspension of 0.45 g of Nafion in dimethylformamide (DMF), prepared as described elsewhere [13]. The mixture was homogenized by a treatment in ultrasonic bath for 2 h. The resulting suspension was recast in a Petri dish with a diameter of 2.5 cm, at 110 °C for 15 h, under a hot air stream. The resulting membranes were: (a) dislodged from the Petri dish by a treatment with hot bidistilled water, (b) partially dried under an air flow at room temperature for 1 h, (c) hot-pressed at T = 100 °C and p = 70 bar for 5 min in order to improve their mechanical properties. The purification and activation of the recast membranes were carried out as follows. The composite membranes were washed in bidistilled water at 80 °C for 1 h. The samples were treated twice with a 3 vol.% solution of H_2O_2 and three times with 1 M H_2SO_4 at 80 °C. Each washing step lasted for 1 h. Afterwards, the materials were washed three times for 1 h at 80 °C in bidistilled water. The membranes were fully hydrated in an autoclave at T = 120 °C, p = 3.3 bar for 30 min. This latter treatment was considered the "reference zero point" of the thermal history of all the Nafion-based composite membranes described in this report. The obtained membranes were stored in bidistilled water at room temperature inside polyethylene terephthalate (PET) bags. A pristine Nafion membrane and a [Nafion/$(Si_{80}F)_{0.7}$] hybrid membrane were prepared starting from 1.5 g of Nafion suspended in DMF, and were recast on a Petri dish with a diameter of 7 cm. These membranes were used to prepare membrane-electrode assemblies (MEAs).

2.4. Water uptake and membrane reference conditions (RC)

The water uptake of fully hydrated nanocomposite films was determined by measuring the TG profiles of the isothermal mass elimination vs. time as reported elsewhere [21]. The number of moles of water per equivalent of acid groups (λ) was determined from the standard TG profiles using Eq. (1):

$$\lambda(t) = 1000 \times \left[\frac{wt(t) - wt(t=\infty)}{wt(t=\infty) \cdot MW_{H_2O} \cdot \chi_{Nf} \cdot f_{Nf}} \right] \quad (1)$$

where wt(t) and wt($t = \infty$) are the weight of the sample at $t = t$ and t = 100 min, respectively (Fig. 4). MW_{H_2O} is the molecular weight of water, χ_{Nf} [mequiv. g^{-1}] is the PEC of Nafion and f_{Nf} is the weight fraction of the ionomer in the dry membrane. In this report, $\lambda(t)$ is the amount of H_2O present in the membrane at the time t. $\lambda_r(t) = \lambda(t_0) - \lambda(t)$ is the water eliminated by the membrane at the time t. t_0 is the initial instant of the desorption process, calculated as reported elsewhere [21]. The water uptake, which corresponds

to the λ_r value of Fig. 5 at $t = \infty$, was determined as follows. First, water was eliminated from the membrane isothermally at 35 °C for 60 min (Fig. 4). Second, the membrane was heated up to 135 °C, requiring 20 min. Finally, the membrane was kept at the constant temperature of 135 °C for additional 20 min. Thus the water uptake, which corresponds to the total amount of water eliminated from the membrane, was measured after 100 min since the beginning of the experiment.

2.5. Instruments and methods

The morphology of the investigated samples was examined by scanning electron microscopy (SEM) with a Cambridge Stereoscan 250 Mark 1 operating at an acceleration voltage of 25 kV. To ensure the conductivity of the samples, a film of Au with a thickness of 200–300 Å was sputtered on each sample with an Edwards S150A sputterer. Thermogravimetric analyses were carried out with a high-resolution TGA 2950 (TA Instruments) thermobalance. A working N_2 flux of 100 mL min^{-1} was used. The TG profile was recorded in the range of temperature from 20 to 800 °C using an open platinum pan loaded with ca. 7 mg of sample. Modulated Differential Scanning Calorimetry (MDSC) measurements were carried out with a MDSC 2920 Differential Scanning Calorimeter (TA Instruments) equipped with the LNCA low-temperature attachment operating under a helium flux of 30 mL min^{-1}. The measurements were made on ca. 5 mg of sample hermetically sealed in an aluminum pan with a heating rate of 3 °C min^{-1} in the temperature range $-50 < T < 350$ °C with modulation amplitude and period set to 0.954 °C and 60 s, respectively. Dynamic Mechanical Analyses (DMA) were carried out with a TA Instruments DMA Q800, using the film/fiber tension clamp. Temperature spectra were measured by subjecting a rectangular film sample of ca. 25 mm (height) × 6 mm (width) × 0.2 mm (thickness) to an oscillatory sinusoidal tensile deformation at 1 Hz with an amplitude of 4 μm and a preload force of 0.05 N. Measurements were carried out in the temperature range from −10 to 210 °C, at a rate of 4 °C min^{-1}. The mechanical response data were analyzed in terms of elastic (storage) modulus (E'), viscous (loss) modulus (E'') and $\tan\delta = E''/E'$. TG, MDSC and DMA analyses were carried out on samples dried in a flow of dry air at room temperature for 24 h. The measurements of complex conductivity spectra were carried out in the frequency range 10 mHz–10 MHz, using a Novocontrol Alpha-A analyzer. The temperature range from 5 to 155 °C was explored by using a home-made cryostat operating with a N_2 gas jet heating and cooling system. The measurements were performed using a closed home-made cell. This cell allowed to maintain the membrane wet during the measurements as follows: the freshly autoclaved membrane, sandwiched between two circular platinum electrodes, was located inside a cylindrical Teflon cell. The free volume of the cell was partially filled with 100 μL of bidistilled water in order to avoid drying during measurements up to 155 °C. The geometrical constant of the cell was determined by measuring the electrode–electrolyte contact surface; the distance between the electrodes was measured with a micrometer. No corrections for the thermal expansion of the cell were carried out. The temperature was measured with an accuracy less than ±0.02 °C. The absence of water loss during measurements was checked by weighting the closed cell before and after the measurements. The complex impedance ($Z^*(\omega) = Z'(\omega) + iZ''(\omega)$) was converted into complex conductivity ($\sigma^*(\omega) = \sigma'(\omega) + i\sigma''(\omega)$) using the equation $\sigma^*(\omega) = k[Z^*(\omega)]^{-1}$, where k is the cell constant and $\omega = 2\pi f$ (f is the frequency in Hz). The bulk conductivity of the material, σ_{DC} was then determined by measuring the conductivity value interpolated in the plateau of the $\sigma'(\omega)$ profiles at frequencies greater than 10^5 Hz, as described elsewhere [13,24].

2.6. Preparation of membrane-electrode assemblies and tests in a single-cell configuration

Two MEAs were prepared as outlined elsewhere [25] using a hybrid [Nafion/$(Si_{80}F)_{0.7}$] membrane and a recast Nafion membrane obtained as described in Section 2.3. The commercial EC-20 electrocatalyst was acquired by ElectroChem Inc. and was used on both the anodic and the cathodic side of each MEA. The platinum loading on each electrode was ca. 0.4 mg cm^{-2}. The active area of both MEAs was 4 cm^2. The performance of the MEAs was evaluated using pure hydrogen as the fuel and both air and pure oxygen as oxidants. The temperatures of the cell and the gases were 85 and 84 °C, respectively. The hydrogen, air and pure oxygen flow rates were 800, 1700 and 500 sccm, respectively. The back pressure of the fully humidified gases was kept at 4 bar. Single-cell tests were carried out in a 5 cm^2 single cell with one-channel serpentine flow-fields for both anodic and cathodic sides. The channels were 1 mm wide and 0.5 mm deep. The plates were made of graphite. MEA performance was determined as follows. Polarization curves were collected continuously from open-circuit potential (OCP) up to 0.1 V at 5 mA s^{-1}, until the system reached stability. The final polarization curve was collected immediately afterward. The polarization curves were not corrected for internal resistance losses.

3. Results and discussion

3.1. Preparation and characterization of $Si_{80}F$ nanofiller

Si_{80} silica was functionalized with HFNO to obtain a hydrophobic nanofiller, labelled $Si_{80}F$, which is characterized by a surface covered with fluorocarbon chains. The latter are expected to ensure a good compatibility between the nanofiller and the fluorocarbon backbone chains of the host polymer. The reaction between the silanol groups on the surface of Si_{80} and HFNO proceeded through acid catalysis as shown in Scheme 1. The PECs of Si_{80} and $Si_{80}F$ were 0.6 and 0.3 mequiv. g^{-1}, respectively. The functionalization degree (ρ_F) of $Si_{80}F$ was expressed as $\rho_F = N_{org}/N_{SiOH}$. N_{org} is the number of organic chains bound to the silica "core" in the $Si_{80}F$ nanofiller; N_{SiOH} is the number of silanol groups on the surface of the Si_{80} precursor. Both N_{org} and N_{SiOH} are expressed per unit mass of material. N_{org} was determined starting from the mass loss event observed between 400 and 600 °C in the TG profile of $Si_{80}F$ (Fig. 1). Indeed, that mass loss event was attributed to the degradation of the fluorocarbon chains present on the surface of $Si_{80}F$. N_{SiOH} is determined from the mass elimination observed in the Si_{80} precursor from 200 to 800 °C in the TG profile (Fig. 1). ρ_F is evaluated from the data

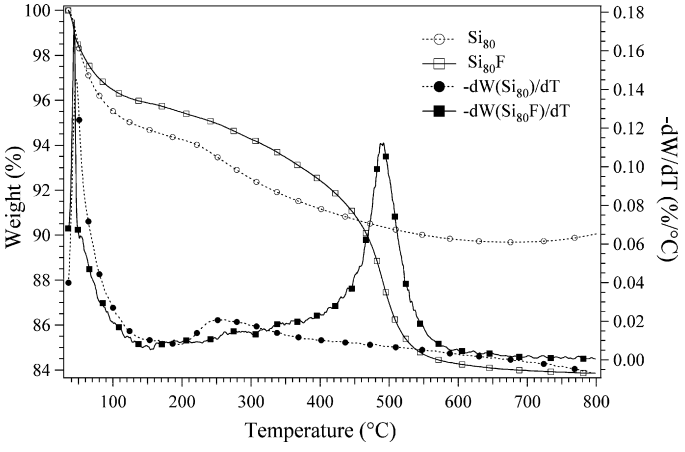

Fig. 1. TG measurements of Si_{80} precursor and $Si_{80}F$ hydrophobic nanofiller.

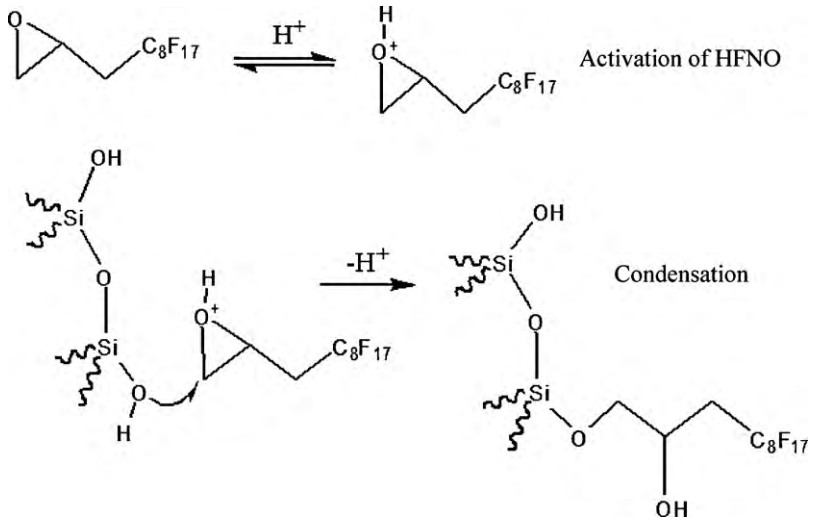

Scheme 1. Reaction mechanism between HFNO and silanol groups of Si_{80}.

derived from TG analysis using Eq. (2):

$$\rho_F(\text{TGA}) = \frac{1000}{100}\frac{\Delta\text{wt\%(org)}}{\text{MW}_{\text{HFNO}}}\frac{1}{N_{\text{SiOH}}} \quad (2)$$
$$\Delta\text{wt\%(org)} = \Delta\text{wt\%}(Si_{80}F) - \Delta\text{wt\%}(Si_{80})$$

Δwt% is the mass elimination of each sample in the temperature range between 400 and 600 °C. The ρ_F value obtained applying this procedure is equal to 0.03. It is to be pointed out that the procedure outlined above can be applied only if the functionalization degree of the nanofiller is very small. In this case the number of silanol groups present on the surface of Si_{80} precursor and on the $Si_{80}F$ nanofiller is essentially the same, and is expressed as N_{SiOH}. N_{org} has also been determined starting from the C assay obtained from elemental analysis. In this case, the calculated functionalization degree ρ_F was equal to 0.035. TG profiles also evidenced that $Si_{80}F$ and Si_{80} are very different in the 200–300 °C temperature range. In this region, Si_{80} shows a characteristic mass loss event attributed to the elimination of water arising from the condensation of neighbouring silanol groups. On the other hand, isolated silanol groups condense at a higher temperature, up to ca. 1000 °C [26,27]. This condensation event is highlighted by the broad peak in the derivative of the Si_{80} TG trace observed at ca. 250 °C. The functionalized $Si_{80}F$ nanofiller does not show such an event clearly, indicating a lower surface concentration of neighbouring silanol groups. This evidence confirms that the functionalization of Si_{80} was successful, and took place preferentially on neighbouring silanol groups. SEM micrographs were collected for both Si_{80} and $Si_{80}F$ (Fig. 2). The images show aggregates in the micrometric range, while nanometric primary particles were not resolved. With respect to $Si_{80}F$, Si_{80} shows larger particle aggregates. This evidence is attributed to the polar interaction between the surface silanol groups of Si_{80} nanoparticles. On the other hand, in the case of $Si_{80}F$ this phenomenon is hindered by the bulky, non-polar perfluorinated chains on the surface of the nanoparticles.

3.2. TGA and DSC analysis of the membranes

The TG profiles of the [Nafion/$(Si_{80}F)_\Psi$] membranes (Fig. 3) showed three main mass loss events. The first event, detected between 240 and 300 °C, was attributed to the degradation of the sulphonyl groups of the Nafion host polymer and is equal to ca. 2–4%. The second and the third events, peaking at ca. 350 and 430 °C, were ascribed to the decomposition of the side and the fluorocarbon backbone chains of Nafion host polymer, respectively. This behaviour is consistent with previous results obtained on other hybrid inorganic–organic Nafion-based materials [13,28]. The temperature of each mass loss event is very similar for all the membranes, so it was concluded that the thermal behaviour of the Nafion host polymer is not significantly affected by the content of $Si_{80}F$ nanofiller. Fig. 4 reports the plot of $\lambda_r(t) = \lambda(t_0) - \lambda(t)$ vs. time. Fig. 5 shows the dependence of the water uptake and $\lambda_{r(t=\infty)}$ vs. Ψ. The pristine Nafion membrane is characterized by

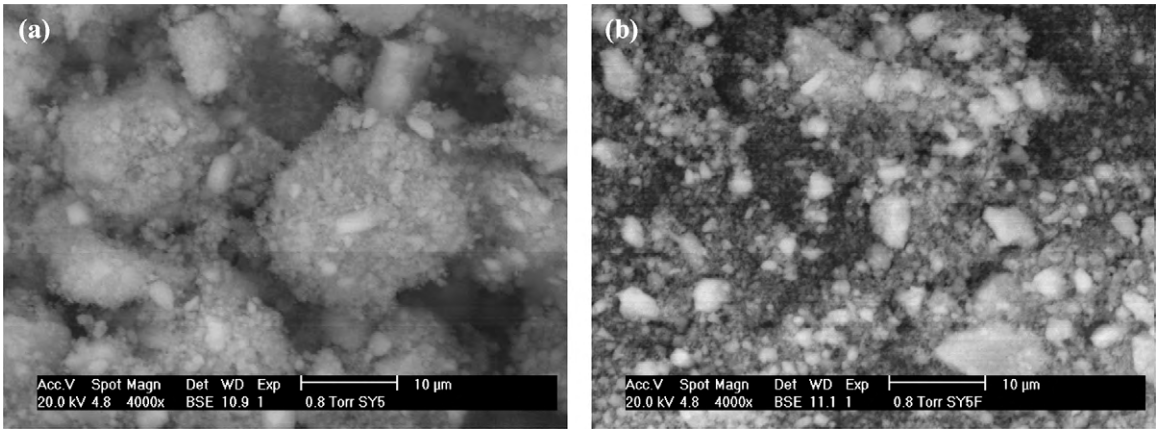

Fig. 2. SEM images collected with backscattered electrons of (a) Si_{80} precursor and (b) $Si_{80}F$ nanofiller.

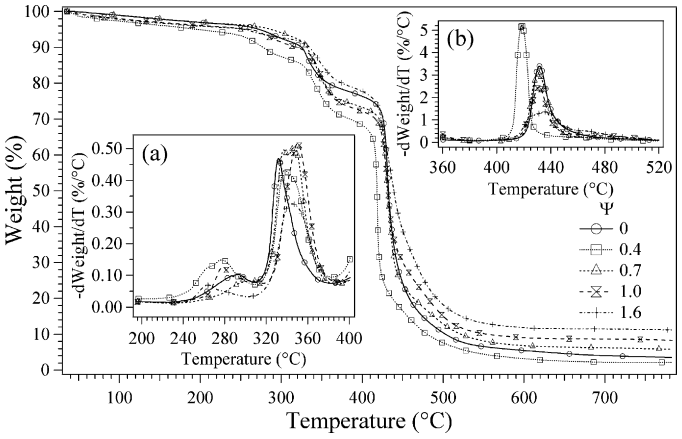

Fig. 3. TG measurements of [Nafion/(Si$_{80}$F)$_{\Psi}$] nanocomposite membranes. The insets show the dependence of the derivative of TG profiles vs. temperature in the regions: (a) 200–400 °C; and (b) 360–520 °C.

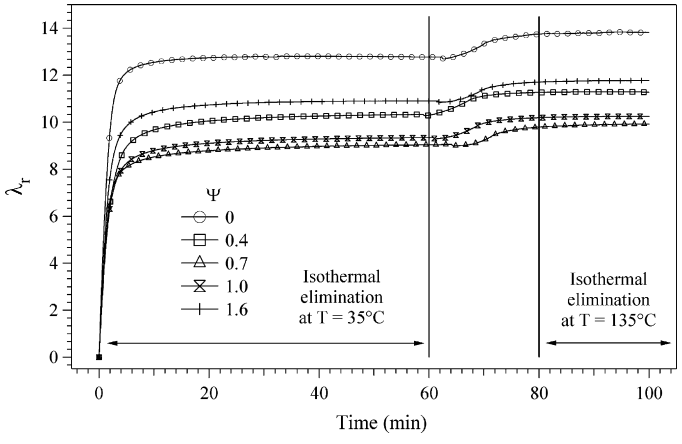

Fig. 4. Dependence of λ_r vs. time for [Nafion/(Si$_{80}$F)$_{\Psi}$] membranes.

a water uptake = 23.2%, corresponding to $\lambda_{r(t=\infty)}$ = 13.9. All the [Nafion/(Si$_{80}$F)$_{\Psi}$] membranes are characterized by a lower water uptake (Fig. 5). This evidence is attributed to the hydrophobic character of Si$_{80}$F nanofiller. The water uptake showed a minimum at Ψ = 0.7, with water uptake = 17 wt.% and $\lambda_{r(t=\infty)}$ = 9.9. The increase in water uptake and $\lambda_{r(t=\infty)}$ observed at Ψ > 0.7 was ascribed to a progressive phase segregation between the nanofiller and the Nafion host polymer, giving so rise to weaker polymer–silica interactions. The MDSC profiles of all the [Nafion/(Si$_{80}$F)$_{\Psi}$] hybrid membranes evidence two main endothermal transitions between

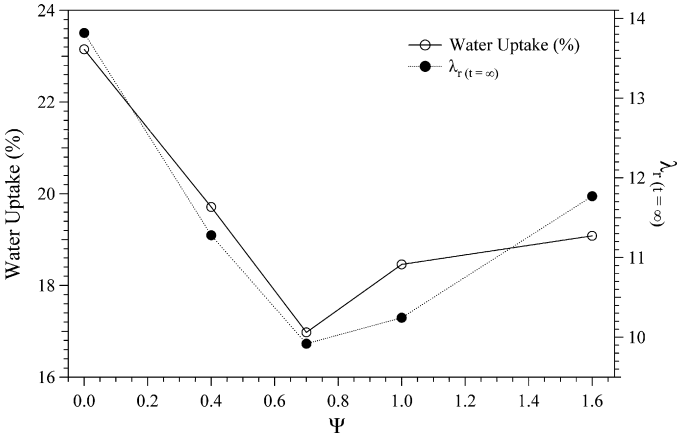

Fig. 5. Dependence of water uptake and $\lambda_{r(t=\infty)}$ vs. Ψ.

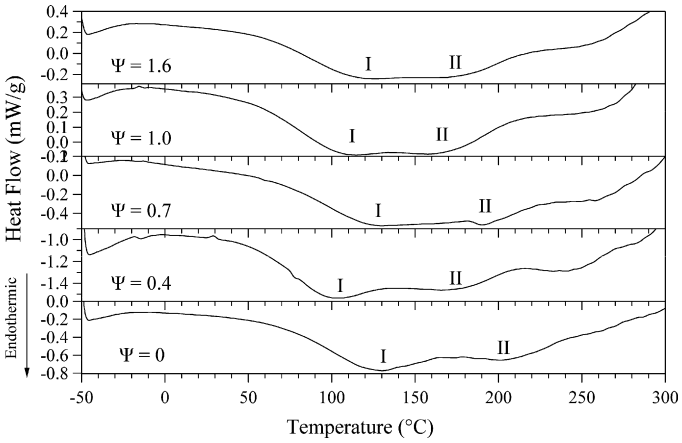

Fig. 6. MDSC curves of [Nafion/(Si$_{80}$F)$_{\Psi}$] membranes in the temperature range −50 to 300 °C. I and II indicate the detected endothermic peaks.

ca. 50 and 250 °C (Fig. 6). The first endothermal peak (I) is attributed to the melting of small and imperfect fluorocarbon nanocrystalline domains of Nafion [22]; the second endothermic peak (II), evidenced between 230 and 250 °C, was assigned to the melting of the microcrystalline domains of Nafion [13,28–31]. A third broad peak characterized by a lower intensity is probably overlapped to peak II and has been attributed to the degradation of the sulfonic acid groups [13]. Indeed, TG analysis points out that the degradation of the sulphonyl groups occur at T > 240 °C. Further information was obtained analyzing how the temperature of the maxima of the two endothermic peaks T_I and T_{II} is affected by Ψ (Fig. 7). In particular: (a) the temperature difference between T_I and T_{II} increases slightly as Ψ is lowered; (b) T_{II} is lower in [Nafion/(Si$_{80}$F)$_{\Psi}$] hybrid membranes with respect to pristine Nafion. The behaviour of the endothermal MDSC peaks can be rationalized admitting that the fluorocarbon chains of the Si$_{80}$F nanofiller interact with the fluorocarbon domains of the Nafion host polymer, decreasing their crystalline size and thus depressing the temperature of the endothermal transitions. This effect is more pronounced for the microcrystalline fluorocarbon domains, revealed by the endothermal peak II.

3.3. DMA analysis of the membranes

DMA analysis provided valuable information on the mechanical properties of materials as a function of temperature; it also allowed to detect thermomechanical relaxations, which have a strong influence on the mechanical and electric properties of the

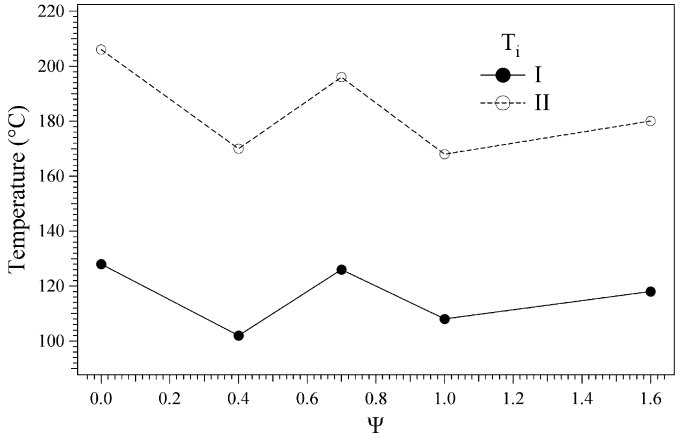

Fig. 7. Dependence of T_I and T_{II} of MDSC endothermic peaks I and II vs. Ψ.

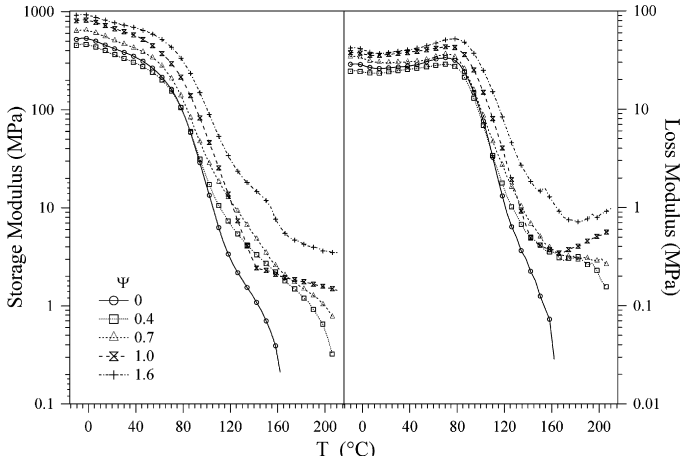

Fig. 8. Temperature spectra of storage (E') and loss modulus (E'') vs. temperature for [Nafion/($Si_{80}F)_\Psi$] hybrid membranes.

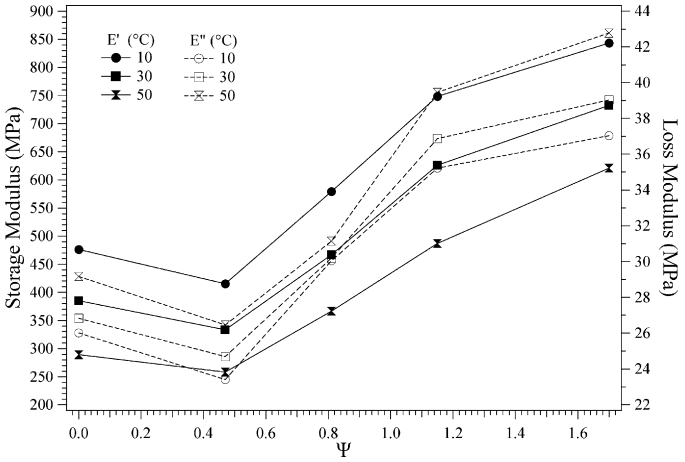

Fig. 10. Dependence of storage (E') and loss modulus (E'') on Ψ for [Nafion/($Si_{80}F)_\Psi$] membranes at selected temperatures.

materials [13]. Fig. 8 shows the dependence of the storage modulus (E') and loss modulus (E'') vs. temperature for [Nafion/($Si_{80}F)_\Psi$] nanocomposite films in the temperature range $-10 < T < 210$ °C. In the temperature range between 0 and 50 °C E' is essentially independent on temperature, while E'' is linearly increasing on T. At higher temperatures E' decreases, while E'' reaches a maximum around $T = 80$ °C and then decreases as well. At 160 °C an irreversible elongation was registered for the pristine recast Nafion membrane, while [Nafion/($Si_{80}F)_\Psi$] nanocomposite films retain a measurable E' up to 200 °C. All the hybrid membranes described in this work are stiffer than pristine Nafion, especially at high temperatures. The tan δ profiles reported in Fig. 9 ($\tan\delta = E''/E'$) evidence one intense peak at ca. 100 °C and a weak shoulder at ca. 50 °C (see inset (a) of Fig. 9). The two events were assigned to the α and β relaxations, respectively. The α mode corresponds to the long-range motion of both the backbone and the side chains, which takes place when a weakening of electrostatic interactions within the ionic aggregates occurs. The β event was attributed to the order–disorder conformational transitions occurring in the hydrophobic PTFE-like domains of the Nafion host polymer [22]. It is observed that E' increases as Ψ is raised (Fig. 10). On the other hand, the intensity of the maximum of the α relaxation peak decreases as Ψ is raised (inset (b) of Fig. 9), implying that a smaller fraction of the overall mechanical energy provided to the system is dispersed by this relaxation mode on Ψ.

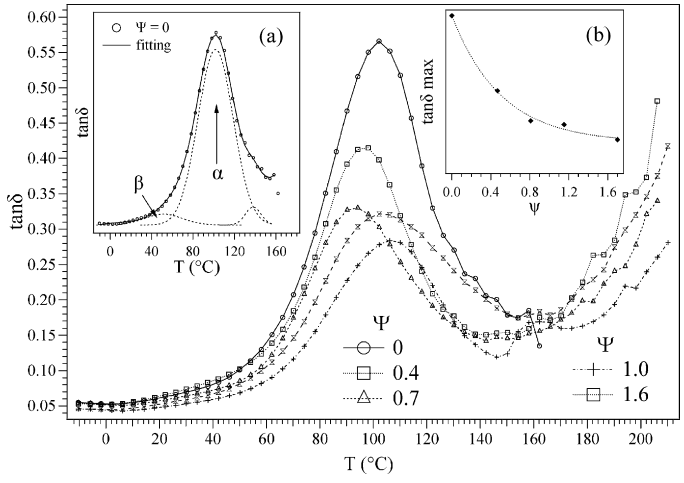

Fig. 9. tan δ vs. temperature of [Nafion/($Si_{80}F)_\Psi$] membranes. The insets show a typical fitting of a tan δ profile (a) and the intensity of maximum tan δ as a function of Ψ (b).

This dual behaviour allows to conclude that the $Si_{80}F$ nanoparticles interact both with the polar domains and with the fluorocarbon hydrophobic domains of the Nafion host polymer. Indeed, the interactions between the sulfonic groups of the Nafion host polymer and residual silanol groups on the surface of the $Si_{80}F$ particles lead to an increase of E' as Ψ is raised. On the other hand the fluorocarbon functional groups on the surface of the nanofiller act to plasticize the hydrophobic domains of Nafion host polymer, thus decreasing the intensity of the α relaxation peak and the size of the hydrophobic fluorocarbon domains of Nafion. It can be concluded that, with respect to pristine Nafion, the hybrid [Nafion/($Si_{80}F)_\Psi$] nanocomposite films show better mechanical properties at higher temperatures.

3.4. Electric conductivity measurements

Selected $\sigma'(\omega)$ vs. frequency plots are shown in Fig. 11. The profiles can be divided in two regions: at a frequency lower than ca. 10^5 Hz, $\sigma'(\omega)$ increases as the frequency is raised; at higher frequencies, a $\sigma'(\omega)$ plateau is reached. This behaviour is consistent with dielectric studies carried out on other polymer electrolytes [32–36], where the $\sigma'(\omega)$ vs. frequency spectra were divided in three regions. The first is dominated by electrode polarization phenomena and corresponds to the region below 10^5 Hz in Fig. 11. The second is characterized by a $\sigma'(\omega)$ plateau, whose value corresponds to the effective direct current conductivity of the sample

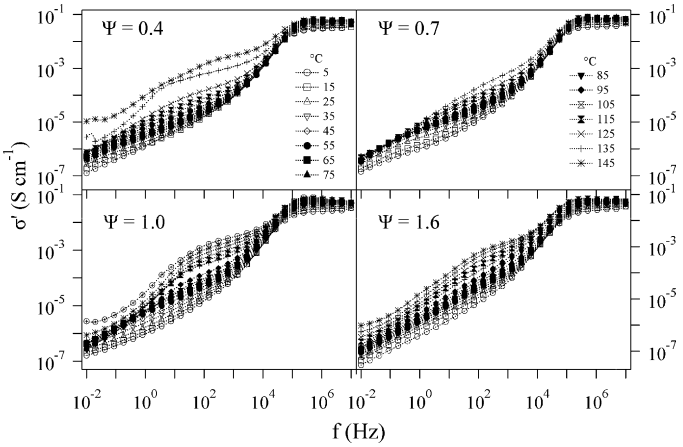

Fig. 11. Spectra of the real component $\sigma'(\omega)$ of the complex conductivity for selected [Nafion/($Si_{80}F)_\Psi$] membranes.

(σ_{DC}). The third region is found at higher frequencies and is not visible in Fig. 11; it is usually characterized by increasing values of $\sigma'(\omega)$. In conclusion, the σ_{DC} value at RH = 100% of [Nafion/$(Si_{80}F)_{\Psi}$] membranes was measured by averaging the values of $\sigma'(\omega)$ in the high-frequency plateau of each isothermal profile. The resulting values were used to study the temperature dependence of the conductivity (Fig. 12). The shape of the σ_{DC} vs. $1/T$ profiles is similar for all the materials at $T < 100\,^{\circ}C$. All the samples show similar conductivity values. The exception is [Nafion/$(Si_{80}F)_{0.7}$] which is the most conductive material in the investigated temperature range. The conductivity value of [Nafion/$(Si_{80}F)_{0.7}$] is noteworthy as this membrane is characterized by the lowest water uptake of the whole series. In addition, with respect to pristine Nafion, the proton conductivity of the other [Nafion/$(Si_{80}F)_{\Psi}$] membranes is not affected by their lower water uptake values. The dependence of σ_{DC} vs. Ψ may be explained taking into consideration the plasticizing action of the $Si_{80}F$ nanofiller. The latter prompts the segmental motion of the hydrophobic fluorocarbon chains of the Nafion host polymer, thus promoting the long-range charge migration through a peristaltic-like process [13]. At higher Ψ values and $T < 80\,^{\circ}C$, the effect of charge carrier dilution in the hybrid materials becomes relevant and explains the lower σ_{DC} values of the [Nafion/$(Si_{80}F)_{1.0}$] and [Nafion/$(Si_{80}F)_{1.6}$] membranes. Furthermore, the conductivity behaviour of the hybrid membranes becomes significantly different, with respect to pristine Nafion, at $T > 100\,^{\circ}C$. Indeed, the conductivity of [Nafion/$(Si_{80}F)_{\Psi}$] materials increases monotonically over a wider temperature range, thus leading to a wider stability range of conductivity (SRC) [13,22]. In particular, [Nafion/$(Si_{80}F)_{1.0}$] shows a monotonic increase in conductivity up to $155\,^{\circ}C$, thus reaching a maximum value equal to $0.08\,S\,cm^{-1}$. This effect has been attributed to the improved thermal and mechanical stability which characterize this family of materials. It is observed that the conductivity of pristine Nafion begins to decrease at a temperature corresponding to the α relaxation detected by DMA. This phenomenon in hybrid membranes is progressively inhibited as the nanofiller concentration rises. In conclusion, in the pristine Nafion the drop in the conductivity is sharply influenced by the structural transitions occurring in the fluorocarbon domains, while the mechanical and electric properties of the hybrid membranes are quite independent on these phenomena owing to the stabilizing effect of $Si_{80}F$ nanoparticles.

3.5. Tests in a single-cell configuration

The polarization curves of the MEAs assembled with the [Nafion/$(Si_{80}F)_{0.7}$] membrane and a pristine recast Nafion membrane are shown in Fig. 13. The thickness of each proton conducting membrane and the figures of merit of MEA performance are reported in Table 2. Both MEAs mounted the same electrodes and gas diffusion layers, were assembled according to the same protocol and were tested in the same operating conditions, which were intended to reduce as much as possible the reagent transport limitations. In conclusion, the performance of the prepared MEAs is mainly differentiated by the proton conductivity of the membranes. It is observed that, with respect to the MEA assembled with the pristine recast Nafion membrane, the MEA based on the hybrid [Nafion/$(Si_{80}F)_{0.7}$] membrane provides an improved performance both in terms of maximum power density and in terms of current density at 0.65 V, using both air and pure oxygen as oxidants (Table 2). These evidences are consistent with a lower proton resistance of the [Nafion/$(Si_{80}F)_{0.7}$] membrane, which is slightly thicker with respect to the pristine recast Nafion membrane used to assemble the reference MEA. It should be pointed out that the area-specific resistance (ASR) values, determined considering the membrane thicknesses (Table 2) and the conductivity data at $85\,^{\circ}C$ (Section 3.4), measured with the membranes immersed in bidis-

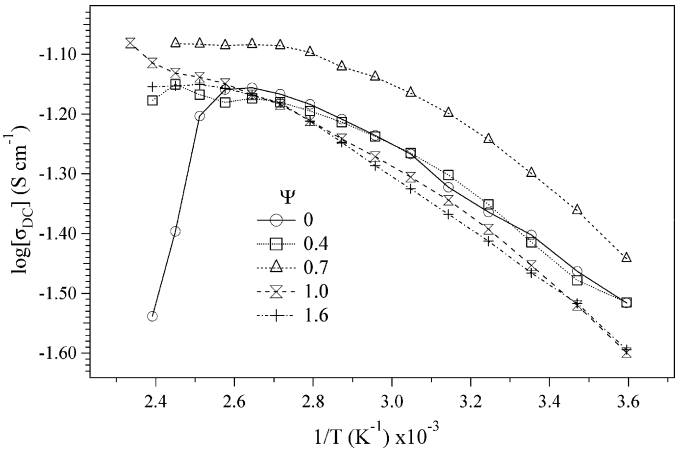

Fig. 12. Dependence of $\log \sigma_{DC}$ vs. $1/T$ for [Nafion/$(Si_{80}F)_{\Psi}$] membranes.

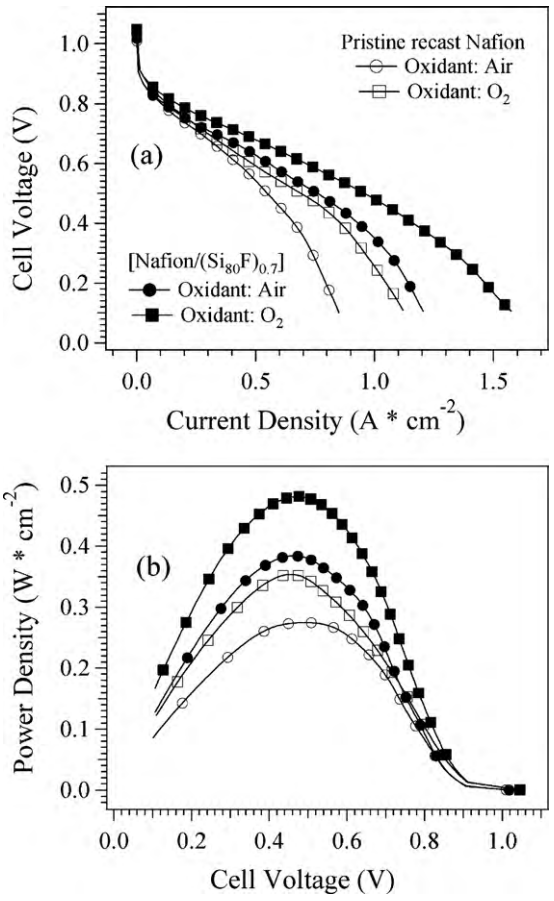

Fig. 13. (a) Polarization curves; and (b) power curves obtained from MEAs assembled with a recast pristine Nafion membrane (open symbols) and the [Nafion/$(Si_{80}F)_{0.7}$] hybrid membrane (solid symbols).

Table 2
Thickness of membranes and main figures of merit of MEA performance.

Membrane	Recast Nafion	[Nafion/$(Si_{80}F)_{0.7}$]
Thickness (μm)	150	180
Maximum power density ($W\,cm^{-2}$)	Air: 0.27 O_2: 0.35	Air: 0.38 O_2: 0.48
Current density at 0.65 V ($A\,cm^{-2}$)	Air: 0.352 O_2: 0.392	Air: 0.448 O_2: 0.575

tilled water, resulted 0.232 and 0.224 $\Omega\,cm^2$ for the pristine recast Nafion and the [Nafion/$(Si_{80}F)_{0.7}$] membrane, respectively. The ASR values determined between 0.4 and 0.7 V in the polarization curves (Fig. 13) resulted 0.54 and 0.36 $\Omega\,cm^2$ for pristine recast Nafion and the [Nafion/$(Si_{80}F)_{0.7}$] membrane, respectively. The comparison of ASR values thus determined allowed to assess that: (a) the performance difference of materials expected from conductivity measurements is negligible; (b) the ASR values obtained in polarization curves were at least 50% larger with respect to those determined from conductivity measurements; and (c) the ASR value for the [Nafion/$(Si_{80}F)_{0.7}$] membrane is ca. 67% of that of the pristine recast Nafion membrane determined from the polarization curves. Results allowed to affirm that, as the membranes are immersed in water, the interstitial free water in bulk materials reduces the differences of conductivity existing between the various proton conducting systems. Indeed, the free water flooding the interconnecting channels provides a significant contribution to the overall proton migration mechanism. However, when the membranes are equilibrated with water vapour, as in the case of the polarization curves, the λ of the materials is lower and depends on the interaction of water molecules with the functional groups present at the interfaces of the different nanocomponents. Therefore, with respect to the materials immersed in water, a higher ASR value of membranes is expected. Taken together, with respect to the pristine recast Nafion, the [Nafion/$(Si_{80}F)_{0.7}$] membrane showed a lower water uptake, an improved thermal stability and a fuel cell performance not affected by lowering of the relative humidity down to 50% (data not shown). For these reasons, it is realistic to consider [Nafion/$(Si_{80}F)_{0.7}$] as a promising candidate for applications in PEMFCs operating at high temperature and low relative humidity.

4. Conclusions

This report presents the results of studies carried out on hybrid [Nafion/$(Si_{80}F)_{\Psi}$] systems intended to explore the effects of the interactions between the Nafion host polymer and a hydrophobic filler on the thermal, mechanical and electric properties of the resulting nanocomposite materials. A hydrophobic filler labelled $Si_{80}F$ was prepared by an acid-catalyzed reaction between nanometric sized silica and fluorocarbon oxirane HFNO. The functionalization degree of the product $Si_{80}F$ was determined by thermogravimetric measurements and was equal to 3% of the silanol groups of the precursor. The resulting $Si_{80}F$ nanofiller showed a hydrophobic behaviour, with a PEC of 0.3 mequiv. g^{-1}, i.e., one half with respect to the Si_{80} precursor. Thermal analyses carried out on $Si_{80}F$ confirmed that the functionalization reaction occurred successfully. $Si_{80}F$ was used in the preparation of a set of five hybrid inorganic–organic membranes with a filler concentration ranging from 0 to 10 wt.%. TGA analyses revealed that the thermal stability of the membranes is independent on the filler content and that the onset of the first degradation event is around 220 °C. The introduction of the hydrophobic nanofiller reduced the water uptake of the hybrid membranes. The lowest water uptake was registered for the [Nafion/$(Si_{80}F)_{0.7}$] material. The I and II thermal transitions revealed by MDSC analysis were associated to the melting of small and imperfect fluorocarbon domains and to the melting of fluorocarbon microcrystalline domains of the Nafion host polymer. The temperature of these transitions decreased as Ψ was raised due to the plasticizing effect of the hydrophobic nanofiller. DMA showed an increase in E' for the hybrid membranes. This observation is attributed to the formation of crosslinks between the surviving silanol groups of the $Si_{80}F$ nanofiller and the sulfonic acid groups of the Nafion host polymer. This effect is particularly evident at high temperatures. DMA also revealed a decrease on Ψ of the intensity of the α mode in tan δ profiles, which demonstrates the plasticizing effect of the hydrophobic nanofiller on the fluorocarbon domains of Nafion. The mechanical stabilization originated from the two types of interaction occurring between the $Si_{80}F$ filler and the Nafion host polymer enhances the electric properties of the material. Indeed, the hybrid materials: (a) with respect to pristine Nafion, show a wider stability range of conductivity, $5 \leq T \leq 135$ °C; (b) present σ_{DC} values comparable to that of the pristine recast Nafion membrane, thus demonstrating for the first time that the use of a hydrophobic nanofiller is beneficial in proton conducting materials. Indeed, it should be evidenced that [Nafion/$(Si_{80}F)_{0.7}$], which is characterized by the lowest water uptake, shows the highest conductivity with a maximum value of 0.083 S cm^{-1} at 135 °C. This last result was further confirmed by tests carried out in a single fuel cell, where a MEA built using the [Nafion/$(Si_{80}F)_{0.7}$] membrane reached a maximum power density of 480 mW cm^{-2}, compared to the 392 mW cm^{-2} achieved by the MEA assembled with a pristine recast Nafion membrane in the same conditions. In conclusion, the synthesis of the $Si_{80}F$ hydrophobic nanofiller allowed to prepare hybrid inorganic–organic proton conducting membranes with a remarkable mechanical and thermal stability and with a good proton conductivity, which make them very promising materials for application in PEMFCs.

Acknowledgements

Research was funded by the Italian MURST project PRIN2007 and NUME of FISR2003, “Sviluppo di membrane protoniche composite e di configurazioni elettrodiche innovative per celle a combustibile con elettrolita polimerico”. Dr. Nicola Boaretto would like to thank Texa S.p.a. of Treviso (Italy) for the financial support. The authors are grateful to Dr. Riccardo Gallina and Dr. Ing. Giovanni Zannini of Silysiamont S.p.A. (Milan, Italy) who provided the Si_{80} amorphous silica.

References

[1] J. Larminie, A. Dicks, Fuel Cell Systems Explained, John Wiley and Sons, Chichester, 2000.
[2] K.A. Mauritz, R.B. Moore, Chem. Rev. 104 (2004) 4535–4585.
[3] K.A. Mauritz, Mater. Sci. Eng. C: Biol. S.6 (1998) 121–133.
[4] G. Alberti, M. Casciola, Annu. Rev. Mater. Res. 33 (2003) 129–154.
[5] S. Malhotra, R. Datta, J. Electrochem. Soc. 144 (1997) L23–L26.
[6] B. Tazi, O. Savagodo, Electrochim. Acta 45 (2000) 4329–4339.
[7] B. Tazi, O. Savagodo, J. New Mater. Electrochem. Syst. 4 (2001) 187–196.
[8] K.A. Mauritz, R.M. Warren, Macromolecules 22 (1989) 1730–1734.
[9] B. Baradie, J.P. Dodelet, G. Guay, J. Electroanal. Chem. 489 (2000) 101–105.
[10] W. Apichatachutapan, R.B. Moore, K.A. Mauritz, J. Appl. Polym. Sci. 62 (1996) 417–426.
[11] P.L. Shao, K.A. Mauritz, R.B. Moore, Chem. Mater. 7 (1995) 192–200.
[12] M.B. Satterfield, P.W. Majsztrik, H. Ota, J.B. Benziger, A.B. Bocarsly, J. Polym. Sci. Part B: Polym. Phys. 44 (2006) 2327–2345.
[13] V. Di Noto, R. Gliubizzi, E. Negro, G. Pace, J. Phys. Chem. B 110 (2006) 24972–24986.
[14] P. Costamagna, C. Yang, A.B. Bocarsly, S. Srinivasan, Electrochim. Acta 47 (2002) 1023–1033.
[15] C. Yang, S. Srinivasan, A.S. Aricò, P. Creti, V. Baglio, V. Antonucci, Electrochem. Solid-State Lett. 4A (2001) 31–34.
[16] H. Wang, B.A. Holmberg, L. Huang, Z. Wang, A. Mitra, et al., J. Mater. Chem. 12 (2002) 834–837.
[17] R. Suzhen, S. Gongquan, L. Chennan, L. Zhenxing, W. Zhimou, J. Wie, Q. Xin, Y. Xuefen, J. Membr. Sci. 282 (2006) 450–455.
[18] M. Vittadello, E. Negro, S. Lavina, G. Pace, A. Safari, V. Di Noto, J. Phys. Chem. B 112 (2008) 16590–16600.
[19] V. Di Noto, R. Gliubizzi, E. Negro, M. Vittadello, G. Pace, Electrochim. Acta 53 (2007) 1618–1627.
[20] V. Di Noto, S. Lavina, E. Negro, M. Vittadello, F. Conti, M. Piga, G. Pace, J. Power Sources 187 (2009) 57–66.
[21] V. Di Noto, M. Piga, L. Piga, S. Polizzi, E. Negro, J. Power Sources 178 (2008) 561–574.
[22] V. Di Noto, M. Piga, S. Lavina, E. Negro, K. Yoshida, R. Ito, T. Furukawa, Electrochim. Acta, in press, doi:10.1016/j.electacta.2009.06.011.
[23] W.L.F. Armarego, D.D. Perrin, Purification of Laboratory Chemicals, fourth ed., Butterworth-Heinemann, Oxford, 1996, p. 19.
[24] V. Di Noto, P. Damioli, M. Vittadello, R. Dall'Igna, F. Boella, Electrochim. Acta 48 (2003) 2329–2342.

[25] E. Negro, V. Di Noto, J. Power Sources 178 (2008) 634–641.
[26] L.T. Zhuravlev, Pure Appl. Chem. 61 (1989) 1969–1976.
[27] R.S. Mc Donald, J. Phys. Chem. 62 (1958) 1168.
[28] S.H. De Almeida, Y. Kawano, J. Therm. Anal. Calorim. 58 (1999) 569–577.
[29] T.D. Gierke, G.E. Munn, F.C. Wilson, J. Polym. Sci. Polym. Phys. Ed. 19 (1981) 1687–1704.
[30] M. Fujimura, T. Hashimoto, H. Kawai, Macromolecules 14 (1981) 1309–1315.
[31] H.W. Starkweather Jr., Macromolecules 15 (1982) 320–323.
[32] V. Di Noto, J. Phys. Chem. B 104 (2000) 10116–10125.
[33] V. Di Noto, D. Barreca, C. Furlan, L. Armelao, Polym. Adv. Technol. 11 (2000) 108–121.
[34] V. Di Noto, M. Vittadello, S. Lavina, M. Fauri, S. Biscazzo, J. Phys. Chem. B 105 (2001) 4584–4595.
[35] V. Di Noto, J. Phys. Chem. B 106 (2002) 11139–11154.
[36] A.K. Jonscher, Dielectric Relaxations in Solids, Chelsea Dielectrics Press, London, 1983.